Update lagrangian analysis of soil slopes in FEM

S. Mohammadi & H.A.Taiebat
The University of New South Wales, Sydney, Australia

ABSTRACT
Application of a large deformation method to embankments is presented to study their performance during and after failure. In this research the effect of non-linear geometry on the post failure stability of slopes is highlighted. A finite element program is developed to investigate the changing geometry of slopes during failure by including large deformation in the analysis using the updated Lagrangian method; the capabilities of the method are investigated and presented through examples of slope failure where the magnitudes of crest settlement after failure are evaluated and compared. The validity of this method is investigated by examining various soils with different modulus of elasticity and embankment inclination angles. The results of this study show that slopes with an initial factor of safety of less than one may reach equilibrium after failure due to the slope inclination changes during failure. This has an important application in the stability analysis of slopes and in the safety margin that can be selected for different slopes.

RÉSUMÉ
Dans cet article, l'application d'une méthode en grandes déformation à des remblais est présentée pour étudier sa performance pendant et après une défaillance. L'objectif de cette recherche est de mettre en évidence l'effet non-linéaire de la géométrie sur la stabilité des pentes après rupture avec développement un programme par éléments finis. Des exemples présentés sont pour étudier d'amplitudes du tassement de crête après rupture. La validité de cette méthode est étudiée en examinant divers types de sols et la géométrie. Les résultats de cette étude montrent que les pentes avec un facteur de sécurité initiale inférieur à un peuvent atteindre l'équilibre après rupture lorsque la déclivité des pentes varie en raison de la déformation post-rupture. Cela a une application importante dans l'analyse de la stabilité des pentes et dans la marge de sécurité qui peut être sélectionné pour des pentes différentes.

1 INTRODUCTION

Failure of slopes and embankment dams is a direct potential threat to lives and infrastructures. A slope failure with large deformation is more dangerous and damaging than a failure with limited deformation. Large deformation of embankment dams due to their slope failure may result in their crest settlement. This has a potential for overtopping, which always results in catastrophic failure of dams and environmental disaster in case of waste impoundments.

Hunter (2003) presented records of a large number of slope failures and classified slope failures based on soil types. For soils that are highly strain weakening on shearing, progressive failure may develop very rapidly from a localized failure. This type of failure exhibits little observable pre-failure deformation. In some other cases the progressive strain weakening in soil may develop very slowly, allowing identification of the impending failure, provided monitoring and instrumentation devices are appropriately located and their data properly interpreted. Post failure travel distances tend to be of limited extent at "slow" post failure velocities (Hunter, 2003).

The traditional slope stability method, the limit equilibrium method, cannot predict the deformation of slopes before or during failure but only gives a factor of safety (FoS) against failure. Current application of finite element method in slope stability analysis is also limited to prediction of FoS against failure. Application of this method on slope stability analysis leads to more accurate prediction of FoS when compared to the limit equilibrium methods, and requires fewer assumptions regarding the failure mechanism (Griffiths and Lane, 1999). This method has also been used to evaluate the performance of slopes up to the commencement of failure. However, the method has the potential to predict the deformation of slopes during failure.

Application of finite element method on slope stability analysis started with implementation of elasto-plastic soil models into the method (Zienkiewicz et al., 1975). A finite element slope stability analysis is carried out mainly by shear reduction method (Zienkiewicz et al., 1975) or by overloading of the slope (Zheng et al., 2005). One reduces the shear strength parameters gradually and the other increases the total driving force until failure occurs. The accuracy of the shear strength reduction method and its application in problems involving excavation and fill were verified by Matsui and San (1992) and Griffiths and Lane (1999) in a series of analyses where the results obtained by the method are compared with those given by the traditional limit equilibrium method.

In a finite element stability analysis of slopes, an elastic-perfectly plastic soil model, such as Mohr-Coulomb model, is used to capture the failure of the slopes and also to be able to compare the results of the finite element analysis with those given by the traditional limit equilibrium method. Although the soil stiffness parameters are important if the magnitude of pre-failure deformation is going to be evaluated, these parameters do not affect the factor of safety obtainable by the finite element method.

Finite element method has the potential to predict the deformation of slopes during failure, thereby identify the catastrophic failures with large deformations and failures with small movements. Evaluation of movements during

and after failure requires a large deformation analysis. This type of analysis can take into account the changing geometry of a slope during failure and evaluate the post-failure deformation. The post-failure deformation includes movement of the soil mass from the onset of failure to the stage where the slope reaches stability again, provided that no disintegration of the soil particles occurs. Although large deformation analysis has been employed in slope stability analyses, it has never been used to evaluate the post-failure deformation of slopes. Snitbahan and Chen (1978) were probably the first who considered the effects of large deformation developed before failure on the stability of slopes and concluded that the effect of large deformation on the response of slopes can be significant. Li and Ugai (1998) made a comparison between the results of large deformation analysis and the conventional infinitesimal deformation analysis of slopes up to the onset of failure and reported that a larger factor of safety could generally be achieved by large deformation analysis.

In this paper, the behavior and deformation of slopes and embankments during and after failure are presented using the results of a series of finite element stability analysis of slopes employing large deformation formulations. The formulations have been implemented into a finite element program, AFENA (Carter and Balaam, 1995). This method is validated by investigating the relationship between modulus of elasticity and embankment inclination angles of various soils. The scope of this research is limited to simulation of slow failures and the dynamic and inertia effects of soil mass are not considered.

2 LARGE DEFORMATION ANALYSIS

Slope failure is a large deformation problem where soil in a shear band undergoes significant large strain. The changing geometry of a slope during failure may result in stability of the slope after a small or large deformation occurs, depending on the initial margin of safety of the slope. In the stability analysis of many slopes, such as dam embankments, it is important to estimate the maximum deformations of slopes and embankment that could occur after failure, so that the type of failure and the consequence of failure can be evaluated thoroughly. A large deformation finite element analysis takes into account the effects of nonlinear geometry together with nonlinear material behavior and provides a numerical solution to the problem. In a large deformation analysis the changing geometry of a slope during failure can be captured by the updated Lagrangian formulation, while the rotation of each element is taken into account by the large strain theory. The nonlinear geometry can be treated in the same way as the nonlinear material behavior in the finite element analysis procedure using an iterative scheme.

3 LARGE DEFORMATION FORMULATIONS

In a small deformation finite element analysis the constitutive relation is commonly expressed in terms of the Cauchy stress and strain rates, and stresses at any increment can be related to the incremental stains and the stresses in the previous increment using a standard integration procedure as:

$$\sigma_{ij}^{t+\Delta t} = \sigma_{ij}^{t} + \int_0^{\Delta\varepsilon_{kl}} C_{ijkl}(\sigma,\kappa)d\varepsilon_{kl} \quad [1]$$

In a large deformation analysis the configuration of the body is changing continuously. Therefore the Cauchy stress may not be simply integrated directly by adding the stresses and their increments due to deformation. Before stress integration, the following stress transformation (Jaumann) should be applied to correct stresses and to account for stress objectivity (Belytschko et al., 2000). The objectivity of a tensor means that under a finite incremental step, its components will be independent of any rigid body rotation. The stress increment after introducing the Jaumann stress rate into small strain constitutive equation for a given strain increment will be:

$$\sigma_{ij}^{t+\Delta t} = \sigma_{ij}^{t} + \int_0^{\Delta\varepsilon_{ij}} d\sigma_{ij} = \sigma_{ij} + \int_0^{\Delta\varepsilon_{kl}} \sigma_{ij}d\omega_{jk} + \sigma_{jk}d\omega_{ik} + \int_0^{\Delta\varepsilon_{kl}} C_{ijkl}(\sigma,\kappa)d\varepsilon_{kl} \quad [2]$$

$$\omega_{ij} = \frac{1}{2}\left(\frac{\partial u_i}{\partial x_j} - \frac{\partial u_j}{\partial x_i}\right) \quad [3]$$

In the above equations C represents the stress–strain matrix, σ is the true (Cauchy) stress tensor, ε denotes strain tensor, ω represents the rigid body rotation, u_i denotes the displacement vector.

In the Lagrangian formulation the finite element mesh convects with the material, i.e. the finite element nodes are coincident with material points, unlike the Eulerian mesh where the coordinates of nodes are fixed and only material points change with time (Figure 1). In a Lagrangian mesh the boundary nodes and any point on the interface of two materials remain on the same boundary or interface throughout the analysis of the problem. Also treatment of constitutive equations is straight forward. However deformation of elements with the material results in element distortions leading to a deterioration of the performance of the analysis due to ill-conditioning (Belytschko et al., 2000). Nevertheless, the Lagrangian finite element formulation proves extremely useful in large deformation problems and is most widely used in solid mechanics. Lagrangian tensors are defined with reference to the Lagrangian frame, which is not affected by rigid body rotation. The material derivative of any Lagrangian objective tensors will still remain Lagrangian objective. Therefore, under the Lagrangian objectivity, a tensor will remain unaffected by an observer transformation (Belytschko et al., 2000). Nazem et al (2009) states that for some cases like elastic analysis the

stress-integration schemes used in a small-displacement analysis can also be used directly in a large-deformation analysis and no further changes in stress transformation is required. Hu and Randolph (1998) also used an infinitesimal strain incremental analysis combined with regular updating of coordinates and stated that this approach offers accurate solution for large deformation analysis of offshore foundations. Therefore, the same approach is used in this study.

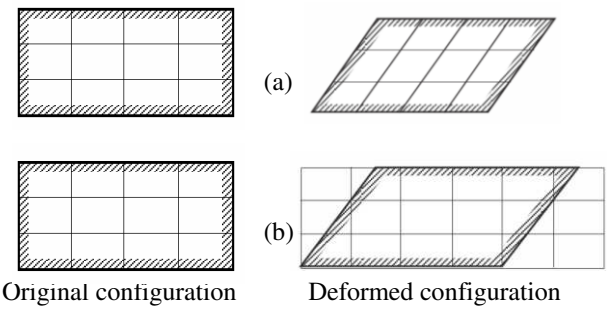

Figure 1: (a) Lagrangian mesh, (b) Eulerian mesh (Belytschko et al., 2000).

4 STRENGTH REDUCTION TECHNIQUE

In the strength reduction technique the FoS of a slope against failure can be evaluated simply by reducing the soil shear strength parameters in a sequence of analyses until collapse occurs. This technique was introduced by Zienkiewicz et al (1975) and has undergone extensive developments since then.

In a finite element stability analysis, the analysis normally commences before failure is initiated, i.e., when the FoS is greater than 1. In this case the mobilized shear stress in the soil is less than the shear strength of soil, i.e. the driving forces and moments which tend to destabilize the slope are smaller than resisting forces and moments. The resisting forces or moments can be reduced by reducing the shear strength parameters. This can be achieved systematically in a finite element analysis by reducing the nominal cohesion, c, and friction angle, ϕ, of the soil by a reduction factor, R (equation 4). The strength parameters used in the analysis will therefore be:

$$c_r = \frac{c}{R}, \qquad \tan\phi_r = \frac{\tan\phi}{R} \qquad [4]$$

where c_r and ϕ_r are the reduced shear strength parameters and R is the shear strength reduction factor. When the strength parameters are reduced to such an extent that the resisting forces or moments become marginally less than the disturbing forces or moments, failure will initiate. It can be seen that at failure *R* will be equal to the factor of safety against failure. This method can be used with any elasto-plastic soil model and with any nominal strength parameters.

In a finite element stability analysis, failure is identified when the algorithm cannot converge within a user-specified maximum number of iterations, i.e. no stress distribution can be found that is simultaneously able to satisfy both the failure criterion and the global equilibrium. In an infinitesimal deformation finite element analysis, slope failure is normally accompanied by a dramatic increase in the displacements of nodes located on the sliding mass within a mesh. However, in a large deformation analysis of slopes, the effects of change in geometry of slopes are taken into account. Even before failure occurs, the change in the geometry of slopes increases the factor of safety slightly. When failure occurs, a slope exhibits much larger deformation which changes the slope angle. As the slope angle reduces the destabilizing forces and moments also reduce and eventually equilibrium will be achieved and the slope becomes stable again. The magnitude of the post-failure deformation will depend on the FoS and the strain softening behavior of the soil; a lower FoS results in a larger crest settlement. In this paper, the effects of strength reduction factor on the magnitude of the post-failure deformation will be presented for two typical slopes.

5 FAILURE IDENTIFICATION

The state of failure in any finite element slope stability analysis needs to be identified so that the factor of safety and/or deformation occurred before failure could be evaluated. In general, shear failure occurs when a mechanism could develop either due to failure of a large number of points or due to formation of a shear band and zones of large strain.

Several possible methods proposed to identify failure, e.g. bulging of the slope profile (Snitbhan and Chen, 1978) limiting of the shear stresses on the potential failure surface (Farias and Naylor, 1998, Kim and Lee, 1997) , concentration of incremental shear strain (Conte et al., 2010) and/or plastic zones (Zheng et al., 2007), visualisation technique (Li, 2007, Griffiths and Kidger, 1995) and non-convergence of the solution (Griffiths and Lane, 1999). The advantages and disadvantages of the different criteria have been discussed by many references (Griffiths and Lane, 1999, Farias and Naylor, 1998, Lechman and Griffiths, 2000), but no resolution was achieved on the superiority of any of the methods.

The criterion based on bulging of the slope profile used by Snitbhan and Chen (1978) considers the change in the states of stress of some points within the slope, when a slope arrives at failure, from elastic states to the states of flow, accompanied by considerable deformations. However the choice of these points and the moment of failure flow are subjective and user dependent.

A criterion based on limiting shear stress is introduced by Farias and Naylor (1998), and Kim and Lee (1997) In this method the shear strength, $[\tau]$, at any point on a user defined failure surface is calculated based on the actual stress field at the point and the shear strength parameters of the soil. The actual stress field is evaluated by FE analysis. A factor of safety is calculated by integrating the

shear strength and shear stress along the pre-defined failure surface. The minimum factor of safety is then evaluated by optimizing the location of the pre-defined failure surface.

$$FoS = \min_{s \in S} \frac{\int_s [\tau] ds}{\int_s \tau ds} \quad [5]$$

where τ is the shear stress at any point in the field which cannot be greater than the limiting shear strength of the soil at the point, which is denoted by $[\tau]$ here.

Zheng et al (2007) discusses that development of plastic zones cannot generally be used as a criterion for failure in all analysis. In most cases, the elastic-perfectly plastic model over-presents failed zones in the finite element slope stability methods. This is due to the transfer of that part of stresses exceeding the residual shear strength to other elements, causing them to fail. The overestimated plastic zones usually undergo very small plastic deformation and can be identified by filtering plastic strains to a limited value (Zheng et al., 2007).

The incremental shear strain can also be used as a criterion for failure of slopes (Conte et al., 2010). When failure occurs, plastic shear strains will continuously develop only along the shear zone. While total cumulative shear strains contain elastic components, and therefore may be distributed over a large area of embankment, the incremental shear strains will be localized around the failure surface. The magnitude of incremental shear strains developed close to convergent state may become too low to allow a clear contouring of the strains.

The non-convergence option is widely taken as an indicator of collapse (Lechman and Griffiths, 2000, Dawson et al., 1999, Griffiths and Lane, 1999). When the finite element algorithm cannot converge within a user-specified maximum number of iterations, the implication is that no stress distribution can be found that is simultaneously able to satisfy both the constitutive model and global equilibrium. If the algorithm is unable to satisfy these criteria, `failure' is said to have occurred. Slope failure and numerical non-convergence occur simultaneously, and are accompanied by a dramatic increase in the nodal displacements within the mesh. However it should be noted that the convergence criterion is controlled by the magnitude of the tolerance of out-of-balance forces and/or the tolerance of nodal incremental displacements, both are specified by the user. Therefore, non-convergence of an analysis does not necessarily mean the collapse of structures.

In the two examples studied here, a criterion based on either incremental or total shear strain is taken as being a suitable indicator of failure in both infinitesimal and large deformation analysis. The critical failure line can be identified by the plot of the contours of the shear strain defined as :

$$\varepsilon = \sqrt{\varepsilon \times \varepsilon}$$
$$\varepsilon = \frac{1}{2}\left(\frac{\partial u_i}{\partial x_j} + \frac{\partial u_j}{\partial x_i}\right) \quad [6]$$

6 LARGE DEFORMATION ANALYSIS OF SLOPES

In this section finite element models for two typical slopes will be presented followed by the results of large deformation finite element simulations of the slopes. The updated Lagrangian method is adopted in the formulation of the finite element analysis. To provide a basis for comparison, the simulation is also performed employing the standard infinitesimal deformation formulation.

The slopes were both simulated in a two-dimensional finite element analysis under plane strain conditions. The soil is assumed to obey the elastic perfectly-plastic Mohr Coulomb failure criterion, with no strain softening behavior. The element type used in the spatial discretization of the slope is the isoparametric 6 noded triangles which have shown superior performance over the 3 noded linear triangular elements. A coarse mesh of 6 noded elements gives a more accurate result than a fine mesh of 3-noded element of equal nodes.

The two slopes considered here are under self weight gravitational loading. The initial stresses due to the soil gravity are distributed in the continuum by simulating staged construction of the slopes.

The solution procedure adopted in the stability analyses is based on the modified Newton-Raphson method using the initial stiffness of the system. Convergence of the finite element solution is established on the basis of the standard Euclidian norm of the out-of-balance forces with a tolerance of 10^{-8}.

6.1 Example 1: General slope failure

A 10 m high homogeneous embankment with a slope of $H:V=2:1$ resting on a 6 m layer of homogeneous soil stratum is considered in this example. The soil is assumed to have a friction angle of $\phi = 20^{o}$, and a stability number of $c/\gamma H = 0.05$. The Young's modulus of the soil is taken as $E = 2000$ kN/m^2, so that the displacement factor of $E/\gamma H^2$ becomes equal to 1. An associated flow rule is used in the analysis with a dilation angle equal to the friction angle of the soil. The geometry of the slope and the finite element mesh used in the analysis is presented in Figure 2. The factor of safety of the slope against failure, evaluated by the infinitesimal deformation stability analysis, is equal to 1.38.

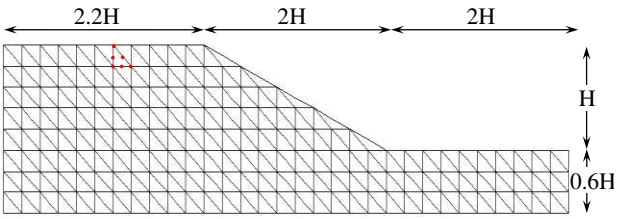

Figure 2. Geometry and finite element mesh of the slope (on homogenous stratum.)

Figure 3 shows contours of the incremental shear strains predicted by the infinitesimal deformation finite element analysis at failure. The crest settlement continuously increases since no equilibrium could be achieved. The infinitesimal deformation finite element analysis exhibits unlimited deformation for any strength reduction factor greater than R=1.38 i.e. any FoS less than 1. However, the large deformation formulation includes the changing shape of the slope during failure and can predict the final displacement of the slope before equilibrium is achieved.

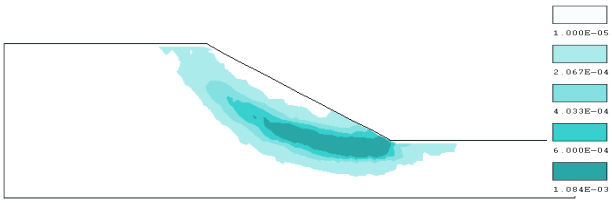

Figure 3. Distribution of the incremental shear strains developed in the slope at failure, infinitesimal deformation analysis.

The deformed shape of the slope predicted by the large deformation analysis under a strength reduction factor of R =1.453 is shown in Figure 4. This reduction factor reduces the shear strength of the soil to such an extent that the initial factor of safety of the slope becomes equal to 0.95 and therefore failure is initiated. Figure 4 clearly shows that the slope surface is still predominantly straight but bulging occurred at the toe of the slope.

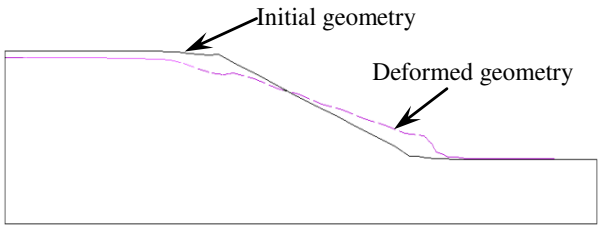

Figure 4. Deformed shape of the slope with FoS=0.95, large deformation analysis.

Contours of the incremental shear strains, predicted by the large deformation analysis under an initial FoS of 0.95, is shown in Figure 5. The incremental strains correspond to iteration number 400, which indicates limited deformation of the slope but progressing toward stability due to continues change in the slope geometry. This figure shows that the failure surface is extended below the toe of the embankment but does not interact with the artificial boundary set at the base of the stratum. Contours of the cumulative shear strain are also shown in Figure 6. It shows a shear band which is identical to that predicted by contours of the incremental shear strain (Figure 5).

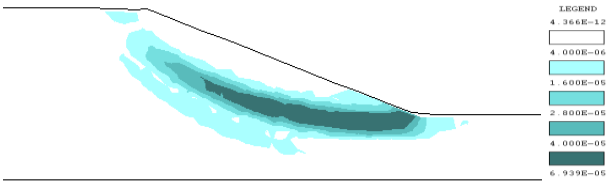

Figure 5. Distribution of the incremental shear strains developed in the slope during failure, FoS=0.95, iteration No=400.

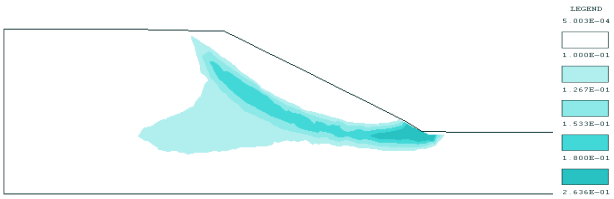

Figure 6. Distribution of the total shear strains developed in the slope during failure, FoS=0.95, iteration No=2400.

A series of large deformation analyses were performed with factors of safety vary from 0.975 to 0.90. The results of the analyses are compared with those of the infinitesimal deformation analysis in Figure 7. In this figure, δ represents the vertical displacement of a point on the crest of the slope. The post-failure crest settlement of the slope with an initial FoS of 0.95 predicted by the large deformation analysis is about δ=0.208 m, after which the slope becomes stable. The crest settlement increases to δ=0.45 m when the initial FoS is reduced to 0.9. The post-failure inclination angle of slope is about 25.5. This angle corresponds to the stable state, with a FoS =1, based on a limit equilibrium analysis.

The infinitesimal deformation formulation clearly leads to erroneous solution by overestimating the displacement after failure. The large deformation formulation includes the change in the geometry and the inclination angle of the slope, which reduces the destabilizing forces and moment gradually. This leads to smaller deformation after the initial failure, as compared to that predicted by the infinitesimal analysis. The magnitude of the deformation predicted by the large deformation analysis is sufficiently large to change the inclination angle of the slope to a stable angle again.

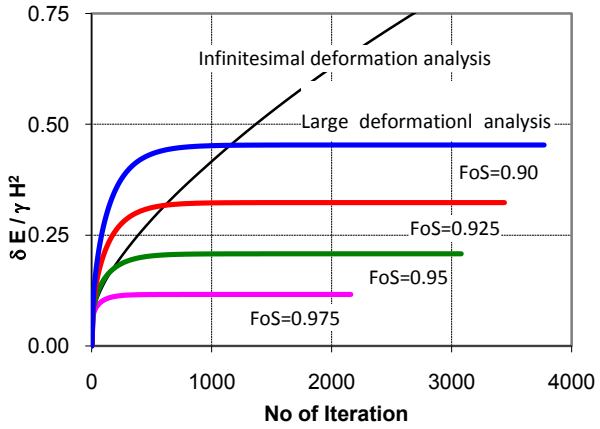

Figure 7. Comparison of crest settlements predicted using large deformation and infinitesimal deformation formulations.

The variation of the post failure crest settlement versus the initial factor of safety is shown in Figure 8. These settlements do not include the initial settlement due to self weight of the soil during the construction stage.

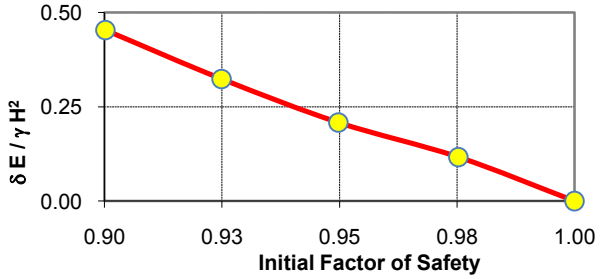

Figure 8. Post-failure crest settlement versus the initial factor of safety, large deformation analysis.

6.2 Example 2: Deep seated failure

This example considers a geometrically similar slope to the previous example but with different material properties so that a different failure pattern, i.e., deep seated failure, can develop during failure. The soil composed of soft soil and is assumed to have a friction angle of ϕ =0°, and a stability number of $c/\gamma H$ =0.222. The Young's modulus of the soil is taken as E =2000 kN/m^2, so that the displacement factor of $E/\gamma H^2$ becomes equal to 1. The factor of safety of the slope against failure, evaluated by the infinitesimal deformation stability analysis, is equal to 1.38.

Contours of the incremental shear strains during failure of the slope with an initial FoS of 0.875 obtained from the large deformation analysis, is presented in Figure 9. The concentration of the contours of high shear strain represents a shear band and also shows the location of the failure zone. This failure zone coincides with the one predicted by the infinitesimal deformation finite element analysis. Note that the incremental shear stains developed along the failure surface is not uniform, unlike those of the previous example. This may be due to the fact that different portions of the critical surface become plastic at different stages of analysis. The distribution of the total shear strains developed during the analysis is presented in Figure 10. Comparing this figure with Figure 9, it is clear that both can be used to identify failure surface. However, a more continuous failure surface may be obtained by the contours of the cumulative shear strains shown in Figure 10.

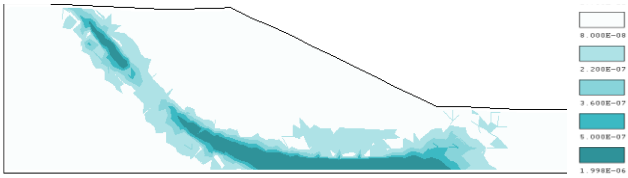

Figure 9. Distribution of the incremental shear strains developed in the slope during failure, FoS=0.875, iteration No=400.

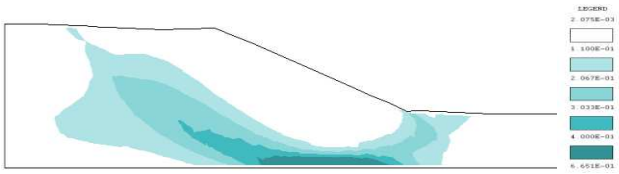

Figure 10. Distribution of the total shear strains developed in the slope during failure, FoS=0.875, iteration No=500.

The large deformation analysis of the slope shows limited deformation before equilibrium is achieved. Figure 11 shows the deformed geometry of the slope for the case where a reduction factor of R = 1.55 is considered. This reduction factor reduces the initial FoS of the slope to 0.95 and therefore initiates failure. However, after a deformation of about δ=0.23 m, the slope becomes stable again.

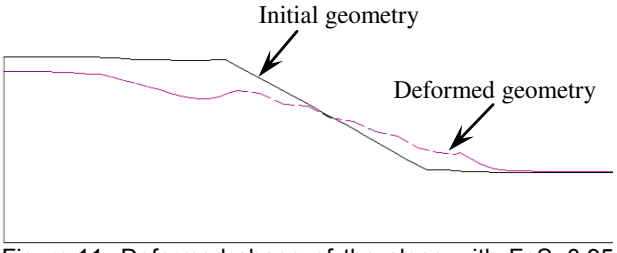

Figure 11. Deformed shape of the slope with FoS=0.95, large deformation analysis.

A series of large deformation analyses were performed with factors of safety vary from 0.975 to 0.90, the results of the analyses are compared with those of the infinitesimal deformation analysis in Figure 12. Unlike the

large deformation analyses which lead to convergence and equilibrium, the infinitesimal deformation analysis shows a large crest settlement without achieving equilibrium.

The crest settlement of the slope with an initial FoS of 0.95 predicted by the infinitesimal deformation analysis approaches δ=1.02 m after 7000 iterations and increases with further iterations. However, the large deformation analyses converge at smaller crest settlements depend on the magnitude of the initial FoS. For a FoS of 0.95 the maximum crest settlement is limited to δ=0.23 m after which the slope becomes stable. The crest settlement increases to δ=0.41 m when the initial FoS is reduced to 0.875. When equilibrium is achieved at the completion of a large deformation analysis, the FoS of the slope with the new geometry will be equal to one.

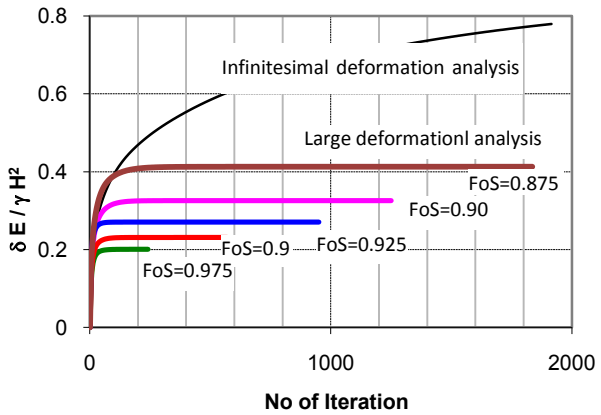

Figure 12. Comparison of crest settlements predicted using large deformation and infinitesimal deformation formulations.

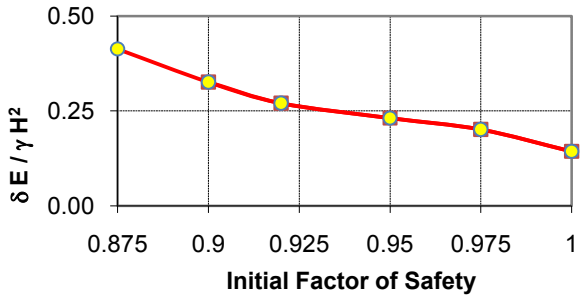

Figure 13. Post-failure crest settlement versus the initial factor of safety, large deformation analysis.

Figure 13 shows the variation of the post-failure crest settlement predicted by the large deformation analyses versus the initial FoS of the slope. In general, the slope modeled in this example requires smaller post-failure deformation to stabilize again, as compared to the slope of the previous example. This is not unexpected since the geometrical requirements for re-stabilization of the two slopes are dependent on the strength parameters, c and ϕ, assumed for the slopes.

7 VALIDATION

In any standard finite element analysis, the deformation predicted is directly proportional to the stiffness parameter assumed for the soil; that is the Young's modulus if Mohr-Coulomb constitutive model is used. In a large deformation analysis of a slope, the stable post failure geometry should be independent of the soil stiffness, but a function of the initial factor of safety of the slope which is related directly to the soil strength parameters. This is verified by a series of analyses performed using different values of Young's modulus, E, for soil. Figure 14 shows the results of the analyses, presented in the form of the slope angle (geometry) vs E, for the two examples described previously. This figure clearly shows the independence of the final geometry to the soil stiffness parameters, thereby validating the solution procedure. The slight variation of the slope angle predicted using different values of E is due to the different initial elastic settlements under the self weight of the soil.

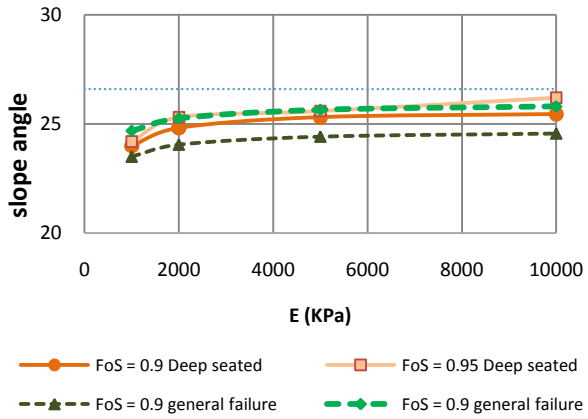

Figure 14. Post-failure slope angle (degrees) versus modulus of elasticity in general and deep seated slope failure, large deformation analysis.

8 CONCLUSIONS

In this paper the behavior of slopes and embankments during and after failure are presented using large deformation finite element analysis. The updated Lagrangian formulation was used together with the strength reduction technique to find the maximum crest settlement of the slopes after failure when the slopes become stable again due to changes in their geometry. Failure was initiated by reducing the shear strength of the soil to such an extent that the initial factor of safety becomes less than unity. In this case, an infinitesimal finite element analysis showed unlimited deformation and the solution did not converge. However, the large

deformation analysis converged after limited deformation. The magnitude of the post failure deformation, predicted by the large deformation analysis, depends on the initial factor of safety, the smaller the initial factor of safety, the larger the post-failure crest settlement. It was also shown that the post failure deformation of the slope is not a function of the stiffness parameters of the soil, but the initial factor of safety of the embankment. In other words, the post failure geometry of a slope is a function of the strength parameters of the soil only.

In the study presented in this paper, the initial factor of safety was reduced, by reducing the shear strength parameters of the whole embankment, to initiate failure. In reality, the reduction in shear strength of strain-softening soils is a function of the mobilized shear strain on the failure surface. A more realistic solution could have been achieved if an appropriate model for the behavior of strain softening soils was incorporated into the analysis. Application of these modes in a large deformation slope stability analysis would capture the post-failure deformation of the sliding mass more accurately.

9 REFERENCES

BELYTSCHKO, T., LIU, W. K. & MORAN, B. 2000. *Nonlinear Finite Elements for Continua and Structures*, John Willey and sons.

CARTER, J. P. & BALAAM, N. P. 1995. AFENA – Users' Manual. University of Sydney, Australia.

CONTE, E., SILVESTRI, F. & TRONCONE, A. 2010. Stability analysis of slopes in soils with strain-softening behaviour. *Computers and Geotechnics,* 37**,** 710-722.

DAWSON, E. M., ROTH, W. H. & DRESCHER, A. 1999. Slope stability analysis by strength reduction. *Geotechnique,* 49**,** 835-840.

FARIAS, M. M. & NAYLOR, D. J. 1998. Safety analysis using finite elements. *Computers and Geotechnics,* 22**,** 165-81.

GRIFFITHS, D. V. & KIDGER, D. J. 1995. Enhanced visualization of failure mechanisms by finite elements. *Computers & Structures,* 55**,** 265-268.

GRIFFITHS, D. V. & LANE, P. A. 1999. Slope stability analysis by finite elements. *Geotechnique,* 49**,** 387-403.

HU, Y. & RANDOLPH, M. F. 1998. A practical numerical approach for large deformation problems in soil. *International Journal for Numerical and Analytical Methods in Geomechanics,* 22**,** 327-350.

HUNTER, G. 2003. *The pre and post deformation of slope.* PhD, UNSW

KIM, J. Y. & LEE, S. R. 1997. An Improved Search Strategy for the Critical Slip Surface using Finite Element Stress Fields. *Computers and Geotechnics,* 21**,** 295-313.

LECHMAN, J. B. & GRIFFITHS, D. V. Year. Analysis of the progression of failure of earth slopes by finite elements. *In*, 2000. 250-265.

LI, Q. & UGAI, K. 1998. Comparative study on static and dynamic sliding behaviors of slopes based on small and large deformation theories. *Soils and Foundations,* 38**,** 201-207.

LI, X. 2007. Finite element analysis of slope stability using a nonlinear failure criterion. *Computers and Geotechnics,* 34**,** 127-136.

MATSUI, T. & SAN, K.-C. 1992. Finite element slope stability analysis by shear strength reduction technique. *Soils and Foundations,* 32**,** 59-70.

NAZEM, M., CARTER, J. P., SHENG, D. & SLOAN, S. W. 2009. Alternative stress-integration schemes for large-deformation problems of solid mechanics. *Finite Elements in Analysis and Design,* 45**,** 934-943.

SNITBHAN, N. & CHEN, W.-F. 1978. Elastic-plastic large deformation analysis of soil slopes. *Computers & Structures,* 9**,** 567-577.

ZHENG, H., LIU, D. F. & LI, C. G. 2005. Slope stability analysis based on elasto-plastic finite element method. *International Journal for Numerical Methods in Engineering,* 64**,** 1871-1888.

ZHENG, H., LIU, D. F. & LI, C. G. 2007. On the Assessment of Failure in Slope Stability Analysis by the Finite Element Method. *Rock Mechanics and Rock Engineering,* 41**,** 629-639.

ZIENKIEWICZ, O. C., HUMPHESON, C. & LEWIS, R. W. 1975. Associated and non-associated visco-plasticity and plasticity in soil mechanics. *Geotechnique,* 25**,** 671-689.